Propagation Failure in an Array of Oregonator Cells and Irreversible Thermodynamics of an Assembly of Discrete Systems

Daniel Barragán

Departamento de Química, Facultad de Cienceias, Universidad Nacional de Colombia, Bogota, Columbia

Byung Chan Eu*

Department of Chemistry and Centre for the Physics of Materials, McGill University, 801 Sherbrooke St. West, Montreal, Quebec H3A 2K6, Canada

In this paper we report on a numerical study of wave propagation and its failure in a one-dimensional array of coupled chemical cells and irreversible thermodynamics of the array. The Oregonator model for the Belousov−Zhabotinsky reaction is used to model the chemical reactions. In particular, we investigate the dependence of wave front propagation failure on the mass exchange rate for the Ce^{4+} component between cells and on the amplitude of a perturbation employed to trigger a propagation of transition from an initially homogeneous state to final stationary patterns reached by the system. In the case of the Oregonator, there appear two critical mass transfer rates at which propagation failure occurs, in contrast to the cases of the cubic model or the sine-Gordon model reported in the literature. By following the evolution of the calortropy production accompanying wave propagation, we construct phase diagrams that provide valuable insights into the propagation failure phenomenon. The global calortropy production is shown to exhibit discontinuous changes with respect to the transfer rate when propagation failure occurs. When a complete propagation failure occurs, the global calortropy flux through the array vanishes, whereas it is nonvanishing when there is a partial or complete propagation of the wave front. When the calortropy flux vanishes, the wave front speed and the net mass flux between the cells also vanish.

I. Introduction

In a recent paper[1] we have applied the method of irreversible thermodynamics of finite systems[2] to study a chemical neural network[3−6] consisting of finite discrete bistable subsystems (continually stirred tank reactor, CSTR) in which oscillating chemical reactions occur while the subsystems (CSTR) interact by exchanging matter between them at a prescribed rate. In ref 1, by suitably fixing the intersubsystem exchange rate of matter according to Hebb's rules of learning,[7] it was possible to make a neural network perform logic operations; we also examined the mode of energy-matter dissipation, namely, calortropy productions accompanying various logic operations by applying the theory of irreversible thermodynamics formulated for neural networks. We believe that the systems and processes therein, either biological or physical, consisting of discrete subsystems must be subject to the laws of thermodynamics, just as local irreversible processes[8−10] are, according to the currently accepted natural philosophy. In ref 1 we have found that there are *characteristic* calortropy productions associated with the logic operations performed by the neural network mentioned.

The aforementioned formulation of the theory was in fact the first step in our study of irreversible thermodynamics of processes in an assembly of discrete subsystems of a finite size, which interact with each other by some means; for example, by exchanging energy or matter or both. In this work we continue the study and apply the theory formulated in another direction: namely, wave propagation in an assembly of discrete chemical reactors (cells) and irreversible thermodynamics accompanying the wave propagation and, in particular, the calortropy production, associated with wave propagation and its failure.

Biological and physiological systems may be regarded, from the viewpoint of irreversible thermodynamics, as consisting of an assembly of the aforementioned discrete subsystems (cells), and many examples of wave propagation therein have been observed experimentally. Calcium waves in living cells,[11] propagation of action potentials in the heart,[12,13] and propagation of pulses in myelinated fibers[14] are typical examples. It has also been observed that wave propagations fail under certain circumstances, giving rise to a breakdown of the systems accompanied by fatal consequences;[15] examples would be demyelinating disease (multiple sclerosis), ventricular fibrillation, and possible cardiac failure. Direct quantitative experimental observations of the propagation failure in living systems is difficult to make. It consequently has motivated some authors to use model systems to study the phenomenon; examples are linear or circular arrays of coupled CSTRs[16−18] and linear arrays of Chua electrical circuits.[19] These experiments and simulations have shown that wave propagation failure occurs if the coupling (e.g., exchange rate of mass or electric charge transfer) between cells (subsystems) is lower than a threshold value.

On the other hand, through a mathematical study of dynamics in arrays of coupled cells Keener[12] has shown that local continuous models, which employ continuum mechanics equations, such as local reaction−diffusion equations, cannot account for the propagation failure phenomenon occurring below the threshold value of the coupling constant and has determined a relation between the wave front velocity and the minimum value of the coupling constant below which the wave propagation fails. Since then, dynamical models in arrays of discrete cells have been theoretically studied by using the Cubic model,[17,20,21] the Lorenz oscillator model,[22] the sine-Gordon potential model,[23] and a piecewise linear reaction model.[24] These theoretical studies have determined the conditions for wave front propagation, the

* Corresponding author. Also at School of Physics, Korea Institute for Advanced Study, Seoul, Korea. E-mail address: Byung.Eu@McGill.Ca.

10.1021/jp012854r CCC: $22.00
Published on Web 01/19/2002

speed of the wave front, and its relation with the coupling between cells. It also has been demonstrated[25] that propagation failure can occur if the propagation medium is inhomogeneous. In the experimental and theoretical works done until now the appearance of a propagating front has been limited to a fixed boundary condition (forced propagation).

In this work, the thermodynamic theory of irreversible processes that has been formulated for an assembly of discrete subsystems (neural networks) in a previous work[1,2] is applied to wave propagation phenomena in an assembly of continually stirred tank reactors (CSTR), which interact at a coupling strength. The chemical reactions in the CSTR are modeled by the Oregonator[26] for the Belousov−Zhabotinsky reaction.[27] We briefly discuss the underlying thermodynamic theory of irreversible processes below in order to present some important notions therein, which are necessary for applying the theory.

In the thermodynamic theory of linear irreversible processes developed by de Donder,[28] Meixner,[29] Prigogine,[30] de Groot and Mazur,[31] and many others under the assumption of local equilibrium, the local equilibrium Gibbs relation is assumed for the entropy of the system, which is postulated to obey a local balance equation. The basic hypothesis therefore is that the entropy, originally defined by Clausius[32] for reversible processes or systems at equilibrium, still remains valid and is applicable even if the processes are irreversible and the systems are removed from equilibrium. The local balance equation for such an entropy has a source term which is postulated to be positive semidefinite in order for the second law of thermodynamics to be satisfied. Since the entropy was originally defined only for reversible processes or for systems at equilibrium, the local equilibrium Gibbs relation for the entropy of a system away from equilibrium is logically inappropriate to use for irreversible processes, and careful analysis[8−10] of the second law of thermodynamics has shown that the notion of entropy used for reversible processes can be generalized so that the second law of thermodynamics can be properly expressed in a mathematical form even if the processes are irreversible. Such generalized quantity has been given the name calortropy, which is the equilibrium (i.e., Clausius) entropy extended to irreversible processes in nonequilibrium systems. We explain it a little more specifically in the following: The second law of thermodynamics was originally phrased in terms of cycles or engines of a gross cale. It has been shown[8−10,33] that the second law of thermodynamics can be expressed in the integral form

$$\oint \mathrm{d}\Psi = \oint T^{-1}(\mathrm{d}Q + \mathrm{d}\Xi) = 0 \qquad (1)$$

where the integration is over the cycle suitably described in the space of macroscopic variables including conserved and nonconserved variables, d$Q$and dΞ denote the compensated heat and the uncompensated heat (originally, Clausius's notions[32]), respectively, and Ψ is the calortropy.[10] It is important to note that despite the process being irreversible the cyclic integral is equal to zero. The uncompensated heat dΞ must obey the inequality $\mathrm{d}\Xi \geq 0$ as a mathematical expression for the second law of thermodynamics for an infinitesimal differential process. Therefore, for a differential process making up the cyclic process the second law of thermodynamics is mathematically represented by the differential form

$$\mathrm{d}\Psi = T^{-1}(\mathrm{d}Q + \mathrm{d}\Xi) \qquad (2)$$

where $\mathrm{d}\Xi \geq 0$, the equality holding only for reversible processes or equilibrium. This differential form gives rise to the extended Gibbs relation, when combined with the first law of thermodynamics. This differential form for calortropy, when put into local form, also gives rise to a local balance equation for the local density of calortropy,[10] where the local density of $\mathrm{d}\Xi/\mathrm{d}t$ appears as a positive semidefinite source term, which vanishes as the system reaches equilibrium. Thus we conclude that the source term in the calortropy balance equation must be positive semidefinite if the irreversible processes in question are to be consistent with the second law of thermodynamics. This source term is called the calortropy production. It will be denoted as $(\mathrm{d}\Xi/\mathrm{d}t)_{\mathrm{array}}$ in the present paper. Not only the balance equation thus obtained in turn can be put into a differential one-form in an extended thermodynamic space of local macroscopic variables that includes nonconserved variables, but also the differential one-form thus obtained has a mathematical structure similar to the equilibrium Gibbs relation for the entropy S that is used in equilibrium thermodynamics: for example, $\mathrm{d}S = T^{-1}(\mathrm{d}E + p\mathrm{d}V)$ in the case of a pressure−volume work. The differential form (2) and its local equivalent, the calortropy balance equation, are the starting point of the thermodynamic theory of irreversible processes developed in ref 10, for example.

The aforementioned theory of irreversible thermodynamics enables us to investigate the thermodynamic consequences of propagation failure or, depending on the viewpoint, its thermodynamic cause, by numerically calculating the calortropy production accompanying wave propagation or its failure.

We construct a one-dimensional array of 101 coupled cells where chemical reactions occur according to the Oregonator model.[26] When the cells are initially in a steady state and the coupling constant for the intercellular interactions is appropriate, a local perturbation of a cell sets a wave in motion and the wave front, which represents transition of the state of the cell from a steady state to another, propagates through the array of the cells, leaving behind it cells in another steady-state reached from the initial steady state. In fact, we find that if the coupling constant is within an interval of values, the wave front propagates throughout the entire array, but if it is below the lower critical value or above the upper critical value then the propagation fails in contrast to the previous studies using the cubic and sine-Gordon models[12,17,20−23] where only one, namely, a minimum critical constant, has been observed. We also find that the propagation failure has characteristic discontinuities in the calortropy production. The calculation of the calortropy production seems to indicate that a propagation failure occurs when the system reaches a state that is unable to dissipate (consume) energy and matter for some dynamical reason. Our results show that both localized perturbation and the coupling constant (exchange rate of mass between cells) are the key parameters to consider in order to avoid the propagation failure of a wave front.

This paper is organized as follows. In Section II the theory of irreversible processes in the coupled discrete subsystems is briefly reviewed, mainly for the sake of introducing the definitions and notation. In section III the Oregonator model is also briefly described together with the kinetic equations for the model and the accompanying rate constants. In this section the evolution equations for concentrations are presented for the linear array of coupled CSTRs. In section IV the evolution equations are solved numerically and wave propagation phenomena are studied together with some aspects of their irreversible thermodynamics. Specifically, we calculate the calortropy production associated with the wave propagation and show it to be discontinuous with respect to the coupling constant. When propagation of the wave front fails, the calortropy production in fact diminishes discontinuously, thereby exhibiting

characteristic levels of value as wave propagation progresses in the interval of the exchange rate. Section V is for discussion and concluding remarks.

II. Irreversible Thermodynamics of Coupled Cells

The formalism of irreversible thermodynamics developed previously[1,2] is applied to a system consisting of finite subsystems (e.g., cells) interacting (i.e., connected) with each other in the sense that they exchange matter and energy through their boundaries.

Since the calortropy differential (eq 2) can be given in terms of the rates of change in macroscopic variables obeying their evolution equations in the aforementioned thermodynamic theory of irreversible processes, the integral of the calortropy differential in the space of macroscopic variables is a surface in which the macroscopic state of the system evolves. In the case of the present system irreversible processes in the array of cells therefore evolve on the calortropy surface spanned by species concentrations, temperature, and pressure. In the sense that the calortropy surface is a mathematical realization of the thermodynamic laws, such processes described by the theory mentioned above are consistent with the thermodynamic laws, which particularly demand that the calortropy production[9] be positive and vanish at equilibrium only. Since the irreversible processes evolve in the calortropy surface, it will be interesting to understand what the consequences will be for the calortropy production for the global system, which also indicates a measure of energy and matter dissipation, that is, in this particular case, matter transforming from a useful to a less useful form in given circumstances, when waves propagate or fail to propagate. We calculate the calortropy production under the assumption that the solutions of reacting species in the solvent are ideal.

The calortropy production $(\mathrm{d}\Xi/\mathrm{d}t)_{\mathrm{array}}$ within the cells in the array of cells with no other irreversible processes than chemical reactions is given by the formula[1,8]

$$(\mathrm{d}\Xi/\mathrm{d}t)_{\mathrm{array}} = -VT^{-1}\sum_{s=1}^{\nu}\sum_{l=1}^{m} A_l^{(s)} R_l^{(s)} \tag{3}$$

where V is the volume, T is the temperature, $A_l^{(s)}$ are the affinities of the reactions, and $R_l^{(s)}$ are the reaction rates. In this expression for the calortropy production the contribution of cell s is summed over all cells in the array. The subscript l stands for reactions and there are m reactions in each cell.

If chemical reactions are the only irreversible processes present in the system, the calortropy production happens to be identical in form with the entropy production appearing in the theory of irreversible processes[30,31] based on the local equilibrium hypothesis, but the calortropy production in the generalized thermodynamic theory of irreversible processes is, rigorously speaking, not the same as the entropy production in the linear theory of irreversible processes mentioned earlier, but a more general notion valid for irreversible processes at any degree of removal from equilibrium of the system. For this reason we keep the terminology of calortropy and calortropy production in this work.

The chemical reactions in cells are the same throughout the array. The rate $R_l^{(s)}$ of reaction l in the cells can be expressed in terms of forward rate Λ_l^+ and reverse rate Λ_l^-:

$$R_l^{(s)} = \Lambda_l^+ - \Lambda_l \tag{4}$$

in accordance with the mass action law. Furthermore, if we denote by $x_{a,s}$ the excess concentrations of species a beyond those in the cells which are in the same thermodynamic state so that there is no material exchange between the cells, and if the chemical potentials are assumed to be those of ideal solutions as is generally assumed in the literature, the chemical potentials of species a can be expressed as

$$\hat{\mu}_a^{(s)} = \hat{\mu}_a^{0(s)} + k_{\mathrm{B}}T \ln x_{a,s} \tag{5}$$

where $\hat{\mu}_a^{0(s)}$ is the chemical potential for the homogeneous state (i.e., the standard state) with regard to species a throughout the array. In other words, the cells are in equilibrium with respect to species a in such a condition. Note that in such a state

$$\hat{\mu}_a^{0(s-1)} = \hat{\mu}_a^{0(s)} = \hat{\mu}_a^{0(s+1)}$$

for all s. Then the aforementioned calortropy production for the array of cells may be written in the form

$$(\mathrm{d}\Xi/\mathrm{d}t)_{\mathrm{array}} = V\mathscr{R}\sum_{s=1}^{\nu}[\sum_{l=1}^{m}(\Lambda_l^+ - \Lambda_l^-)\ln(\Lambda_l^+/\Lambda_l^-)]_s \tag{6}$$

where $\mathscr{R}$ denotes the gas constant. To derive this equation we have made use of the relation between the chemical equilibrium constant, which is equal to the ratio of the forward and reverse rate constants of the reaction. On summing the cell contributions in the square brackets over the array of cells, the total calortropy production arising from the chemical reactions in the entire system is obtained.

In the case of an array of cells in which cells are coupled by exchanging matter between them, there are also contributions to the global calortropy production of the array that arise from the material exchange (the compensated heat) between the cells. This global contribution is given by[1,2]

$$\left(\frac{\mathrm{d}Q_c}{\mathrm{d}t}\right)_{\mathrm{array}} = -T^{-1}\sum_{s=1}^{\nu}\sum_{a=1}^{r}\hat{\mu}_a^{(s)}\frac{\mathrm{d}_e M_a^{(s)}}{\mathrm{d}t} \tag{7}$$

where $M_a^{(s)}$ is the mass of species a in cell s and the symbol $\mathrm{d}_e/\mathrm{d}t$ denotes the transfer time derivative for the rate of change in, for example, $M_a^{(s)}$, that arises from exchange of matter ($M_a^{(s)}$) between cell s and its surroundings. It should be noted that Q_c in this expression does not imply heat, but $(\mathrm{d}Q_c/\mathrm{d}t)_{\mathrm{array}}$ denotes the rate of calortropy change arising from material exchanges between the cells. Since it can be shown that by the mass conservation law within the array

$$\sum_{s=1}^{\nu}\sum_{a=1}^{r}\hat{\mu}_a^{0(s)}\frac{\mathrm{d}_e M_a^{(s)}}{\mathrm{d}t} = 0 \tag{8}$$

the rate of calortropy change associated with the material exchange between the cells through their boundaries is given by the formula

$$\left(\frac{\mathrm{d}Q_c}{\mathrm{d}t}\right)_{\mathrm{array}} = -\mathscr{R}\sum_{s=1}^{\nu}[\sum_{a=1}^{r}\beta(x_{a,s-1} + x_{a,s+1} - 2x_{a,s})\ln x_{a,s}]_s \tag{9}$$

Finally, the total rate of global change in calortropy Ψ in the array of cells is given by the formula

$$\left(\frac{d\Psi}{dt}\right)_{\text{array}} = -\mathcal{R}\sum_{s=1}^{\nu}[\sum_{a=1}^{r}\beta(x_{a,s-1} + x_{a,s+1} - 2x_{a,s})\ln x_{a,s}]_s + V\mathcal{R}\sum_{s=1}^{\nu}\left[\sum_{l=1}^{m}(\Lambda_l^+ - \Lambda_l^-)\ln\left(\frac{\Lambda_l^+}{\Lambda_l^-}\right)\right]_s \quad (10)$$

The terms on the right-hand side of this equation will be abbreviated by the symbols

$$\phi_{\text{net}} = -\mathcal{R}\sum_{s=1}^{\nu}[\sum_{a=1}^{r}\beta(x_{a,s-1} + x_{a,s+1} - 2x_{a,s})\ln x_{a,s}]_s \quad (11)$$

$$\sigma_{\text{net}} = V\mathcal{R}\sum_{s=1}^{\nu}\left[\sum_{l=1}^{m}(\Lambda_l^+ - \Lambda_l^-)\ln\left(\frac{\Lambda_l^+}{\Lambda_l^-}\right)\right]_s \quad (12)$$

It should be noted that σ_{net} is the sum of calortropy productions within cells, whereas ϕ_{net} is the sum over the entire array of calortropy changes arising from the exchange of matter between the cells. The latter should not be regarded as the calortropy production if there is only one cell that exchanges matter with its surroundings, but in the case of an array of cells exchanging matter, the accompanying calortropy change should be included in the calortropy production in the entire array of cells. Therefore, σ_{net} is the volume integral of the cellular calortropy productions over the entire array, whereas $(d\Psi/dt)_{\text{array}}$ is the volume integral of the calortropy over the entire array of cells.

If the concentrations oscillate with a period τ_p, then it is useful to define the mean value of σ_{net} by the time average

$$\sigma_{\text{osc}} = \frac{1}{\tau_p}\int_0^{\tau_p} d\tau\, \sigma_{\text{net}}(\tau) \quad (13)$$

We remark that in the case of a single cell enclosed by its surroundings, the calortropy production is given by σ_{net} only if there are only chemical reactions progressing in the system and ϕ_{net} is just the calortropy flux into or out of the cell or its surroundings. However, if there are coupled cells as is for the present case, then the intercellular interactions and material flow between them must be included in the calortropy production for the whole global system—the global calortropy production. This is one of the major differences between irreversible thermodynamics of a single cell and that of an assembly of cells which is regarded as a single system. Another feature to remember is that the variables involved are uniform over the cellular volume, that is, they are volume averages of local hydrodynamic variables, which are integrated over the cellular volume for the volume averages. For the details of this aspect see ref 2.

III. The Oregonator Model for Chemical Reactions

The system of chemical reactions considered in this work is the Oregonator model,[26] which is based on the Field−Köros−Noyes (FKN) mechanism[27] proposed to explain the oscillatory behavior observed in the Belousov−Zhabotinsky reaction. The values of the kinetic constants are taken from the paper by Gyorgyi et al.[34] The Oregonator model (see reactions CR1−CR6 and Table 1) describes the ceric ion oxidation by bromate ions in a sulfuric acid medium and the oxidative bromination of malonic acid. The system of reactions, when allowed to occur in a CSTR, exhibits a hysteresis between two steady states and thus bistability and oscillations in an interval of values for the control parameter f. Typically, this parameter ranges in our dimensionless version from 0.4769 to 2.1166; see Figure 1. If the value of f is smaller than 0.4769, the steady state is characterized by high concentrations in Ce^{4+} ion (oxidated state), while if the value of f is larger than 2.1166 the steady state is characterized by low concentrations in Ce^{4+} ion (reduced state). At a value between $f = 0.4769$ and $f = 2.1166$, the system makes the transition from one steady state to another because the system is bistable (i.e., because of the presence of the hysteresis loop).

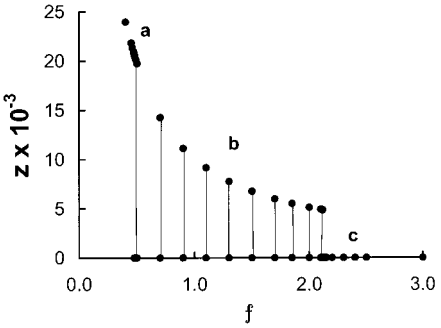

Figure 1. Bifurcation diagram for the Oregonator model. The points in set *a* denote the branch of steady states of high concentrations in the *z* (Ce^{4+}) component (oxidated state); the points in set *b* denote the states in the region of oscillatory behavior ($0.4769 \le f \le 2.1166$), the lines indicating the amplitude of the oscillation; and the points in set *c* denote the branch of steady states of low concentrations in the *z* (Ce^{4+}) component (reduced state).

TABLE 1: Rate Constants for the Oregonator Model

reaction	forward rate constant	reverse rate constant
O1	$k_1 = 2.1$	$k_{-1} = 3.3$
O2	$k_2 = 2 \times 10^6$	$k_{-2} = 5 \times 10^{-5}$
O3	$k_3 = 2200$	$k_{-3} = 33$
O4	$k_4 = 3 \times 10^3$	$k_{-4} = 1 \times 10^{-8}$
O5	$k_5 = 1$	$k_{-5} = 1 \times 10^{-5}$

The reactions for the Oregonator model obtained from the FKN mechanism are as follows:

$$BrO_3^- + Br^- + 2H^+ \rightleftharpoons HBrO_2 + HOBr \quad (14)$$

$$HBrO_2 + Br^- + H^+ \rightleftharpoons 2HOBr \quad (15)$$

$$BrO_3^- + HBrO_2 + 2Ce^{3+} + H^+ \rightleftharpoons 2HBrO_2 + 2Ce^{4+} \quad (16)$$

$$2HBrO_2 \rightleftharpoons BrO_3^- + HOBr + H^+ \quad (17)$$

$$2Ce^{4+} + CH_2(COOH)_2 + H^+ \rightleftharpoons 2Ce^{3+} + fBr^- + \cdots + \text{other products} \quad (18)$$

These chemical reactions have been abbreviated by the Oregonator model as follows:

$$A + Y \rightleftharpoons X + P \quad (19)$$

$$X + Y \rightleftharpoons 2P \quad (20)$$

$$A + X \rightleftharpoons 2X + Z \quad (21)$$

$$2X \rightleftharpoons A + P \quad (22)$$

$$Z \rightleftharpoons fY \quad (23)$$

where $X \equiv HBrO_2$, $Y \equiv HOBr$, $Z \equiv 2Ce^{4+}$, $A \equiv BrO_3^-$, and $P \equiv HOBr$. To cast the evolution equations for the chemical species of the Oregonator model in a general form, it is convenient to use a unified system of notation. Let us denote

the concentrations by x_i and order them in the following manner:

$$x_1 = X,\ x_2 = Y,\ x_3 = Z,\ x_4 = A,\ x_5 = P$$

The rate constants[34] for this system of reactions are summarized in Table 1, where k_i and k_{-i} denote the rate constants for the forward and reverse reaction of reaction i, respectively.

Then the mass action laws for the forward and reverse reactions, respectively denoted Λ_i^+ and Λ_i^-, are given as below:

$$\Lambda_1^+ = k_1 x_4 x_2, \quad \Lambda_1^- = k_{-1} x_1 x_5$$

$$\Lambda_2^+ = k_2 x_1 x_2, \quad \Lambda_2^- = k_{-2} x_4^2$$

$$\Lambda_3^+ = k_3 x_4 x_1, \quad \Lambda_3^- = k_{-3} x_1^2 x_3$$

$$\Lambda_4^+ = k_4 x_1^2, \quad \Lambda_4^- = k_{-4} x_4 x_5$$

$$\Lambda_5^+ = fk_5 x_3,\ \Lambda_5^- = fk_{-5} x_2$$

In this notation the reaction rates for various species in the model are given by

$$R_1 = \Lambda_1^+ - \Lambda_1^- - \Lambda_2^+ + \Lambda_2^- + \Lambda_3^+ - \Lambda_3^- - 2\Lambda_4^+ + 2\Lambda_4^-$$

$$R_2 = -\Lambda_1^+ + \Lambda_1^- - \Lambda_2^+ + \Lambda_2^- + \Lambda_5^+ - \Lambda_5^- \qquad (24)$$

$$R_3 = \Lambda_3^+ - \Lambda_3^- - \Lambda_5^+ + \Lambda_5^-$$

The evolution of species in an isolated cell is then described by the differential equations

$$\frac{dx_i}{dt} = R_i \quad (i = 1, 2, 3) \qquad (25)$$

where $x_4 = 0.06$ and $x_5 = 1$ are constants; recall that species 4 and 5 are maintained at a fixed concentration in the model considered. If the cell is exchanging matter at the rate k_f with its surroundings which are maintained at a fixed composition (x_i^0: $i \geq 1$), then the rate equations should be written as

$$\frac{dx_i}{dt} = k_f(x_i^0 - x_i) + R_i \quad (i = 1, 2, 3) \qquad (26)$$

If the cells are coupled and in exchange of matter with each other at the rate k_f, as is assumed for the present model, it is necessary to distinguish the cells. For this purpose we affix a superscript (s) on various quantities. Furthermore, the material exchange term should be modified so that material exchanges between neighboring cells are properly described by replacing x_i^0 with the concentrations of the neighboring cells. Thus we obtain the evolution equations for cell s

$$\frac{dx_i^{(s)}}{dt} = k_{fi}(x_i^{(s-1)} - x_i^{(s)}) + k_{fi}(x_i^{(s+1)} - x_i^{(s)}) + R_i^{(s)}$$
$$(i = 1, 2, 3;\ s = 1, 2, \cdots, N) \qquad (27)$$

for which we have assumed a uniform material exchange rate at the cell boundaries, namely, k_{fi} are independent of the cell boundaries. It is possible to make the material exchange rate dependent on the cell boundaries at the expense of simplicity in evolution equations. In the present work, it is assumed that only for species 3 is the exchange rate nonvanishing, that is, $k_{f3} \neq 0$ for x_3 only.

Since it is convenient to work with reduced equations, the following reduced variables and dimensionless parameters are defined:

$$x_{10} = k_1 x_4 / k_2,\ x_{20} = k_5 / k_4,\ x_{30} = k_3 x_4 / k_2,$$

$$x = x_1 / x_{10},\ y = x_2 / x_{20},\ z = x_3 / x_{30}$$

$$\tau = t / t_0,\ t_0 = (k_1 k_3 x_4^2)^{-1/2}$$

$$\alpha_0 = (k_{-2} x_5^2 + 2k_{-4} x_4 x_5)/x_4,\ \alpha_1 = k_1(k_3 x_4 - k_{-1} x_5)/k_2,$$
$$\alpha_2 = \alpha_3 = k_1 k_5 / k_4$$

$$\alpha_4 = k_{-3} k_3 k_1^2 x_4^2 / k_2^3,\ \alpha_5 = 2k_1^2 k_4 x_4 / k_2^2,\ \alpha_6 = k_1 / k_2$$

$$\beta = k_{f3} k_2 / x_4 k_3 \sqrt{k_1 k_3}$$

$$\beta_0 = k_{-2} x_5^2 / x_4,\ \beta_1 = k_{-1} k_1 x_5 / k_2,\ \beta_2 = k_1 k_5 / k_4 + fk_5 k_{-5} / k_4 x_4$$

$$\beta_3 = k_1 k_5 / k_4,\ \beta_4 = fk_3 k_5 / k_2,\ \beta_5 = k_5 / k_4 x_4,$$

$$\gamma_0 = k_1 k_3 x_4 / k_2,\ \gamma_1 = k_{-3} k_3 k_1^2 x_4^2 / k_2^3,\ \gamma_2 = k_3 k_5 / k_2,$$

$$\gamma_3 = k_5 k_{-5} / k_4 x_4,\ \gamma_4 = k_3 / k_2,$$

$$T_x = k_1 (k_1 k_3)^{1/2} x_4 / k_2,\ T_y = k_5 (k_1 k_3)^{1/2} / k_4,\ T_z = k_3 (k_1 k_3)^{1/2} x_4 / k_2$$

Note that x_{10}, x_{20}, and x_{30} are the initial values for x_1, x_2, and x_3, respectively. In this reduction scheme the evolution equations of chemical species of the Oregonator in cell s are given by the dimensionless differential equations

$$T_x \frac{dx_s}{d\tau} = g_x(x_s, y_s, z_s) \text{ for } 1 \leq s \leq N$$

$$T_y \frac{dy_s}{d\tau} = g_y(x_s, y_s, z_s) \text{ for } 1 \leq s \leq N$$

$$T_z \frac{dz_1}{d\tau} = g_z(x_1, y_1, z_1) + \beta\gamma_4(z_2 - z_1) \text{ for } s = 1 \qquad (28)$$

$$T_z \frac{dz_s}{d\tau} = g_z(x_s, y_s, z_s) + \beta\gamma_4(z_{s-1} + z_{s+1} - 2z_s)$$
$$\text{for } 2 \leq s \leq (N-1)$$

$$T_z \frac{dz_N}{d\tau} = g_z(x_N, y_N, z_N) + \beta\gamma_4(z_{N-1} - z_N) \text{ for } s = N$$

where the reduced reaction rates are given by the nonlinear functions of variables x, y, and z

$$g_x(x, y, z) = \alpha_0 + \alpha_1 x + \alpha_2 y - \alpha_3 xy - \alpha_4 x^2 z - \alpha_5 x^2 - \alpha_6 x$$

$$g_y(x, y, z) = \beta_0 + \beta_1 x - \beta_2 y - \beta_3 xy + \beta_4 z - \beta_5 y \qquad (29)$$

$$g_z(x, y, z) = \gamma_0 x - \gamma_1 x^2 z - \gamma_2 z + \gamma_3 y$$

These evolution equations are solved for the concentration evolution until the whole array reaches a uniform steady state after time τ_0. The following initial conditions are taken:

$$x_s(0) = 0,\ y_s(0) = 0,\ z_s(0) = 0,\ s = 1, 2, \cdots, N \qquad (30)$$

Then at that instant of $\tau = \tau_0$ a cell s_0 (the cell at the center in

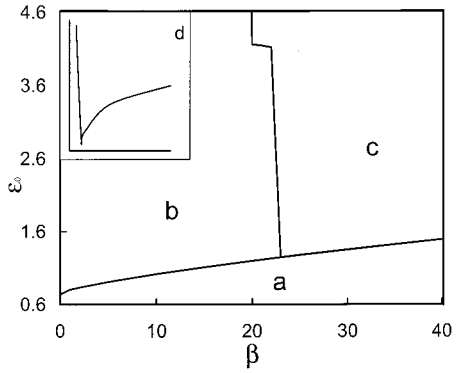

Figure 2. Phase diagram in the plane of the perturbation amplitude ($\epsilon_0 \times 10^{-3}$) and the coupling constant (β) in the case of the wave front propagation when the initial state for the array of cells corresponds to a steady state ($f = 0.4$) in the set *a* of the Figure 1. Region *a* is for wave propagation failure, region *b* is for partial wave propagation, and region *c* is for complete wave propagation. In the inset denoted *d*, a blowup of the lower left corner in the figure is shown, where wave propagation failure occurs if $\beta \lesssim 6 \times 10^{-5}$.

the present work) is perturbed with regard to *z* (ceric ion) by a step function with an amplitude ϵ_0. The concentrations at τ_0 then can be summarized as follows:

$$x_s(\tau_0) = x_{\tau 0}, y_s(\tau_0) = y_{\tau 0} z_s(\tau_0) = z_{\tau 0} + \epsilon_0 \delta(\tau - \tau_0)\delta_{ss0} \quad (31)$$

The perturbation applied to cell s_0 initiates a wave which may propagate through the array. We numerically investigate the mode of wave propagation and the associated calortropy production in this work.

IV. Numerical Results

The systems of ordinary differential equations (eq 28) corresponding to the array of 101 coupled cells are solved numerically with the LSODE[35] subroutine based on Gear's method[36] for stiff ordinary differential equations. We have used a numerically estimated Jacobian matrix and a tolerance between 10^{-8} and 10^{-12} to eliminate spurious numerical data. The array of coupled Oregonators has been studied of its dynamic evolution for the following three distinctive cases of initial steady states of the system. See Figure 1 for the significance of the bifurcation parameter *f* used in the following subsections.

A. Initial Steady State Given by $f = 0.4$ (Oxidated State). The one-dimensional array of coupled Oregonators of $N = 101$ evolves according to the system of evolution equations (eq 28) from the initial state corresponding to a bistable steady state as given by eq 30. The value of the bifurcation parameter *f* of the model is taken $f = 0.4$. When the reduced time reaches $\tau_0 = 1000$, the array has attained a global steady state characterized by a high concentration of the Ce^{4+} ion (oxidated state). At this time the array is perturbed at position $s = 51$, namely, cell 51 is perturbed by an instantaneous pulse according to the conditions (eq 31), and the concentrations of species thenceforth evolve in time ($\tau > 1000$) according to the evolution equations (eq 28). The perturbation then may induce a transition of the perturbed cell to the other stable steady state, and the effect of transition may propagate throughout the array owing to the intricate interactions between nonlinear chemical reactions and material exchange between the cells. For this initial global steady state of the array we have found that only a positive amplitude perturbation ($\epsilon_0 > 0$) is able to trigger a wave front propagation, and the magnitude of the perturbation amplitude varies with the magnitude of the coupling constant β between cells (i.e., exchange rate of mass). Figure 2 shows the phase diagram

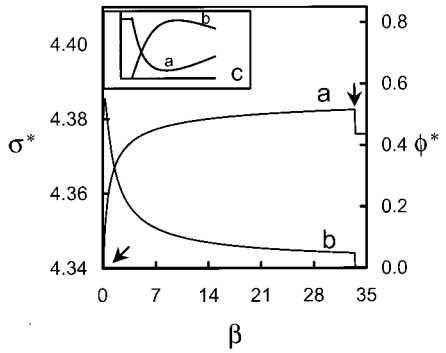

Figure 3. Curve *a* is the global calortropy production ($\sigma^* \times 10^{-3}$) and curve *b* is the global calortropy flux (ϕ^*) as a function of β, when a positive perturbation amplitude (addition of *z*) with value $\epsilon_0 = 1400$ is applied to the array of cells. The phase diagram for this figure is given in Figure 2. The σ^* and Φ^* are given in units of $\mathcal{R}$ according to the definitions $\sigma^* = \sigma_{net}/\mathcal{R}$ and $\phi^* = \phi_{net}/\mathcal{R}$. The inset (c) is a blowup of the figure near $\beta = 0$.

constructed with the minimal value for the perturbation amplitude that is able to trigger a wave front propagation for a given value of the coupling constant β. Since it was discovered that the calortropy production changes discontinuously as a wave front appears and disappears as β is varied, we found it convenient to follow the rate of calortropy change for each cell and construct the phase diagram with the information provided by the calortropy production. It is thus an example of practical use of the calortropy production in the study of the propagation failure problem. Figure 2 shows three different regions in the phase diagram. (a**)** The region where the wave front entirely fails to propagate from the perturbed central cell; we may call this phenomenon complete wave propagation failure. If $\beta \leq 6 \times 10^{-5}$, such wave front propagation failure occurs regardless of the value of ϵ_0. In this case, there is no change in the states of the cells in the entire array. **(**b**)** The region where the wave front propagates until a certain cell is reached−we sometimes will call it partial propagation failure. (c) The region where the wave front propagation occurs throughout the array. It must be noted that wave propagation is unidirectional and irreversible. The phase diagram constructed is useful because it shows the relation between the coupling constant and the minima perturbational amplitude that is able to trigger a wave front. We have explored other values for the bifurcation parameter in this branch of oxidated states (see Figure 1) and have found similar behaviors can be observed if $f < 0.4$, but when the value for *f* is near the bifurcation point $f = 0.4769$, a complex relationship between ϵ_0 and β emerges and a series of wave front propagation failure seems to occur. We will call this a cascade of wave front propagation failure. This phenomenon needs a more thorough investigation. It will be deferred to a later work.

In Figure 3 we show the global calortropy production (σ_{net}) arising from the inherent chemical reactions in the cells and the global calortropy flux (ϕ_{net}) arising from the material exchange between the cells in the array. These quantities change as a function of β for a given value of perturbation amplitude $\epsilon_0 = 1400$. Note that there is an order of magnitude difference between σ_{net} and ϕ_{net}. Consequently, the total calortropy production for the entire array looks similar to curve *a* in the figure. In the region of $\beta < 6 \times 10^{-5}$ where the wave front does not appear, the calortropy production has the same nonvanishing value as that in the region of $\beta \gtrsim 33$ where the propagation also fails. As the wave front appears and propagates through the system as β passes the lower critical value, the calortropy production rises until it suddenly drops as the wave front again fails to propagate at the upper critical value of β in

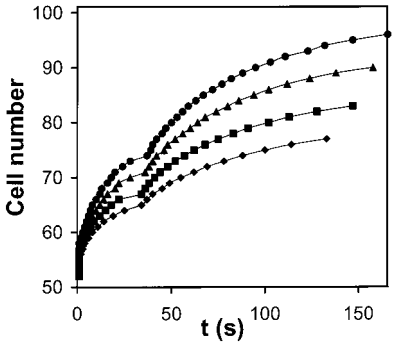

Figure 4. Trajectory of the wave front propagation at different coupling constants: 30 (●), 22.5 (▲), 15 (■), 10 (♦). The initial homogeneous steady state is given by $f = 0.4$ in the set *a* of Figure 1, and the perturbation amplitude by $\epsilon_0 = 1400$.

the neighborhood of $\beta = 33$. Thus the array in the initial thermodynamic state prescribed by the initial conditions as in eq 30 has a characteristic level of global calortropy production in the interval $\beta_{min} \leq \beta \leq \beta_{max}$ where $\beta_{min} \simeq 6 \times 10^{-5}$ and $\beta_{max} \simeq 33$. Unlike σ_{net}, at the upper critical point ϕ_{net} vanishes as it does below the lower critical value of β. The presence of an upper critical value β_{max} of β has not been previously observed in the studies of propagation failure by other authors[12,13,20,17,23] in the literature. It is certainly present in the case of the Oregonator used in this work. The phase diagrams and the discontinuous calortropy production make the presence of such a critical point rather evident. It is noteworthy that the total global calortropy production ($\sigma_{net} + \phi_{net}$) is lower at β approaching β_{max} than in the neighborhood of $\beta = \beta_{min}$, meaning that less energy−matter dissipation is required for a wave to be triggered and propagate near $\beta = \beta_{max}$ than near $\beta = \beta_{min}$ in the present case examined.

In Figure 4 we show the trajectory of wave front as a function of time in the case of four different values of the coupling constant and $f = 0.4$. The shape of the trajectories is qualitatively similar to the experimentally observed shape for the chlorite−iodide system by Laplante and Erneux.[17] Notice the initial rise of the trajectories and the presence of an inflection point at an intermediate time for each curve. We observe there is a kink in each curve, but its origin is not understood at present and it does not seem to arise from the finite size of the array or numerical errors. It may be a manifestation of the region containing the inflection point seen in the data by Laplante and Erneux, because the scales used in the present investigation are by necessity coarse-grained. It is possible to calculate the wave front speed from these curves as a function of the coupling constant.

B. Initial Steady State Given by $f = 1.1$ (Oscillatory Behavior). We now explore the propagation of a wave triggered by a localized perturbation, when the initial global state of the array is oscillatory. The procedure is similar to the one followed in the previous subsection. The global oscillatory state for the array is given by the bifurcation parameter $f = 1.1$. In this case, we have found that only for a positive perturbation amplitude ($\epsilon_0 > 0$) is a particular point (i.e., state) of the limit cycle that describes the oscillatory behavior able to give rise to a wave propagation. More specifically, a small positive amplitude for the perturbation applied at the lowest point (concentration) of the oscillation is able to trigger a wave propagation, whereas at other points on the limit cycle it is practically impossible to trigger a wave propagation with a perturbation with a finite size. When the perturbation is applied to the cell $s = 51$ at the lowest concentration point of the limit cycle, a wave starts to propagate

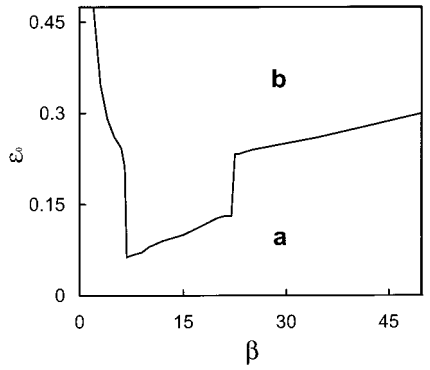

Figure 5. Phase diagram in the plane of β and ϵ_0 for the wave front propagation, when the initial state for the array of cells corresponds to an oscillatory behavior ($f = 1.1$) in the set *b* of Figure 1. Region *a* is for wave propagation failure and region *b* is for complete wave propagation. The positive perturbation (addition of *z*) is applied on the lowest point of the oscillation to generate a wave. The dividing line in the phase diagram means the minimal value in the positive perturbation to obtain wave propagation for a given value of β.

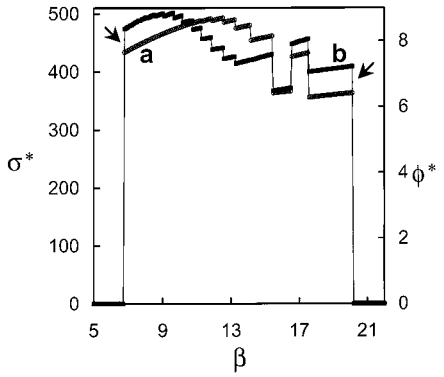

Figure 6. Curve *a* is for the global calortropy production (σ^*) and curve β is for the global calortropy flux (ϕ^*) as a function of *b* when a positive perturbation (addition of *z*) with value $\epsilon_0 = 0.15$ is applied to the array of cells. The phase diagram for this figure is given in Figure 5. The meanings of the symbols are the same as Figure 3.

by destroying the oscillatory motion in each cell, and an amazing variety (a complex stationary pattern) of stable steady states, which are unsymmetrical, emerges. Figure 5 shows the phase diagram constructed with the minimal value for the perturbation amplitude that is able to trigger a wave propagation for a given value of the coupling constant β. The phase diagram shows that in this case a partial wave propagation is not present, but the wave completely propagates throughout the array, if there is a wave triggered. Therefore, we have either a complete wave propagation (region b in the phase diagram) or a complete wave propagation failure (region a in the phase diagram). The phase diagram was constructed by following the calortropy production in a manner similar to the previous subsection. Figure 6 shows the global calortropy production (σ_{net}) arising from the chemical reactions in the whole system and the global calortropy flux (ϕ_{net}) arising from the material exchange between the cells in the system as a function of β for $\epsilon_0 = 0.15$. In Figure 5 for the phase diagram, the propagation failure occurs at $\beta \lesssim 6.8$ and $\beta \gtrsim 20$ if $\epsilon_0 = 0.15$. In this case, the global calortropy production (σ_{net}) and the global calortropy flux (ϕ_{net}) vary in a complex and discontinuous manner in the interval $6.7 \leq \beta \leq 19.9$, exhibiting many discontinuities that are associated with complex patterns emerging in the cells in the wake of the wave front. This means that the complex patterns have characteristic calortropy productions, and this is consistent with a similar observation[37,38] made in connection with pattern formations in

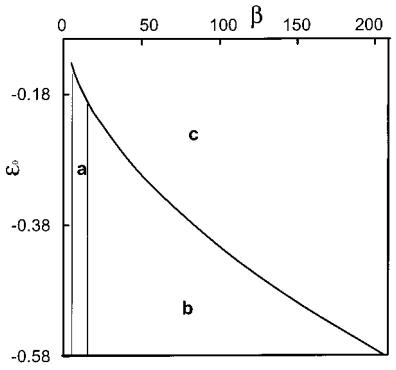

Figure 7. Phase diagram in the plane of β and ϵ_0 for the wave front propagation, when the initial state for the array of cells corresponds to a steady state ($f = 2.2$) in the set *c* in Figure 1. Region *a* is for partial wave propagation, region *b* is for complete wave propagation, and region *c* is for wave propagation failure.

a single cell made up of the Selkov model of chemical reactions. Notice that σ_{net} is again about 2 orders of magnitude larger than ϕ_{net}, and it means that the total global calortropy production for the entire array looks similar to σ_{net}. Again in this case, the total global calortropy production is lower in the region of β_{max} than in the region of β_{min}.

C. Initial Steady State Given by $f = 2.2$ (Reduced State). Finally, we explore the wave front propagation triggered as a result of localized perturbation when the initial global steady state of the array is that specified by the bifurcation parameter $f = 2.2$. This state is characterized by a low concentration of the Ce^{4+} ion (reduced state). The procedure of calculation is similar to the one followed in the previous subsections. Surprisingly, we have found that for this global steady state it is impossible to trigger a wave front propagation with a positive perturbation amplitude for any value of the coupling constant β. This means that the initial state is stable to the perturbation and the system would not make the transition from it to the other stable steady state. However, we have found that a negative perturbation amplitude is able to trigger a wave propagation. Figure 7 shows the phase diagram constructed with the minimal value (taken absolute) for the perturbation amplitude that is able to trigger a wave propagation for a given value of the coupling constant β. The phase diagram was constructed by following the calortropy production in the same manner as for the previous subsections. In this case, the phase diagram is simpler and shows three different regions: (a) partial wave propagation; (b) complete wave propagation; and (c) complete wave propagation failure. In Figure 7 for the phase diagram we see that the propagation failure occurs at $\beta \lesssim 5.3$ and $\beta \gtrsim 38.9$. For $\beta \leq 5.3$, complete wave propagation failure occurs regardless of the magnitude of the perturbation amplitude. Figure 8 shows the global calortropy production (σ_{net}) arising from the chemical reactions in the cells and the global calortropy flux (ϕ_{net}) arising from the material exchange between the cells in the array as a function of β for $\epsilon_0 = -0.28$. In the case considered here, the global calortropy production (σ_{net}) and the global calortropy flux (ϕ_{net}) increase monotonically from a small but nonvanishing value for σ_{net} and from a vanishing ϕ_{net} until a propagation failure occurs at the upper critical value of β where both σ_{net} and ϕ_{net} change discontinuously, the former to a small nonvanishing value and the latter to zero. In contrast to the initial conditions considered in the previous two subsections, the total global calortropy production in the present case is lower at $\beta = \beta_{min}$ than at $\beta = \beta_{max}$.

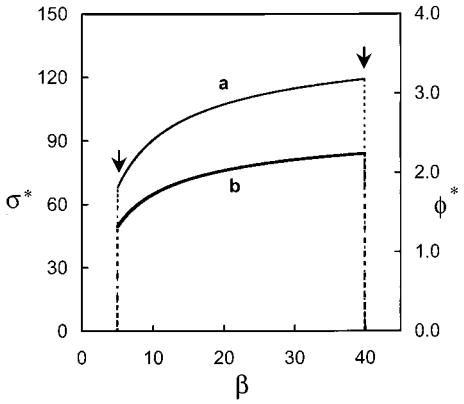

Figure 8. Curve *a* is for the global calortropy production (σ^*) and curve β is for the global calortropy flux (ϕ^*) as a function of b when a negative perturbation (elimination of *z*, e.g., precipitation or complexation) with value $\epsilon_0 = -0.28$ is applied to the array of cells. The phase diagram for this figure is given in Figure 7. The meanings of the symbols are the same as in Figure 3.

V. Discussion and Concluding Remarks

In this work we have numerically explored the conditions to trigger a wave, the wave propagation, and its failure in a linear assembly of 101 interacting cells in which chemical reactions occur according to the Oregonator model. We have also calculated the calortropy production accompanying the phenomena by applying the theory of irreversible processes formulated for networked reactor cells reported previously. The thermodynamic theory of irreversible processes in an assembly of discrete interacting subsystems provides a useful tool for getting insights into this kind of phenomena, for example, by facilitating the construction of phase diagrams. The calortropy production also provides a way to interpret propagation failure in terms of energy−matter dissipation by the system and, perhaps, to optimize wave propagation or, more generally, the irreversible process of interest, with regard to energy−matter dissipation. From the standpoint of irreversible thermodynamics it is possible to view the propagation failure to occur, when the system gets into a state where it is not able to dissipate energy and matter required for the process to evolve into a wave. In any event, since all physical and biological phenomena must be framed within the bounds of the thermodynamic laws, it is necessary to develop a thermodynamic theory of irreversible processes therein, and the present work is an effort toward that end. The propagation failure has attracted the attention of many research workers because of its possible implications in some biological systems. The theory of irreversible thermodynamics presented for an assembly of cells appears to provide an insightful means to investigate various irreversible processes in such systems in a thermodynamically consistent manner, and the wave propagation or its failure examined in this work is an example of application of the theory of irreversible thermodynamics. For example, the sharp changes in calortropy production accompanying propagation failure allow us to find precisely the critical values of control parameters for the wave propagation or its failure. Moreover, since the calortropy surface is an information storage for processes in the system, investigating its mathematical structure might be able provide some useful insights into how the system would behave and wave propagation might arise from the thermodynamic viewpoint. However, a more complete construction of such a calortropy surface would require much more elaborate investigations into the question than what is presented in this paper. It should be left to future work.

Acknowledgment. This work was supported in part by grants from the Natural Sciences and Engineering Research Council of Canada and FCAR of Quebec through the Centre for the Physics of Materials, McGill University. D.B. would like to thank Dr. K. Rah for fruitful discussions in the course of this work.

References and Notes

(1) Barragan, D.; Eu, B. C. *J. Phys. Chem. B* **2001**, *105*, 7104.
(2) Eu, B. C. *J. Phys. Chem.* **1999**, *103*, 8583.
(3) Hjelmfelt, A.; Weinberger, E. D.; Ross, J. *Proc. Natl. Acad. Sci. U.S.A.* **1991**, *88*, 10983.
(4) Hjelmfelt, A.; Weinberger, E. D.; Ross, J. *Proc. Natl. Acad. Sci. U.S.A.* **1992**, *89*, 383.
(5) Hjelmfelt, A.; Ross, J. *Proc. Natl. Acad. Sci. U.S.A.* **1992**, *89*, 388.
(6) Hjelmfelt, A.; Ross, J. *Phys. Chem.* **1993**, *97*, 7988.
(7) Hebb, D. *The Organization of Behavior*; Wiley: New York, 1949.
(8) Eu, B. C. *Kinetic Theory and Irreversible Thermodynamics*; Wiley: New York, 1992.
(9) Eu, B. C. *Phys. Rev. E* **1995**, *51*, 768.
(10) Eu, B. C. *Nonequilibrium Statistical Mechanics*, Kluwer: Dordrecht, 1998**.**
(11) Dawson, S. P.; Keizer, J.; Pearson, J. E. *Proc. Natl. Acad. Sci. U.S.A.* **1999**, *96*, 6060.
(12) Keener, J. P. J. *Theor. Biol.* **1991**, *148*, 49.
(13) de Castro, M.; Hoper, E.; Muñuzuri, A. P.; Gómez-Gesteira, M.; Planck, G.; Schaffehoer, I.; Perez-Muñuzuri, V.; Perez-Villar, V. *Phys. Rev. E* **1999**, *59*, 5962.
(14) Gringrod, P.; Sleeman, B. D. *J. Math. Biol.* **1985**, *23*, 119.
(15) Anderson, A. R. A.; Sleeman, B. D. *Int. J. Bifurcation Chaos* **1995**, *5*, 63.
(16) Marmillot, P.; Kaufman, M.; Hervagault, J. F. *J. Chem. Phys.* **1991**, *95*, 1206.
(17) Laplante, J. P.; Erneux, T. *J. Phys. Chem.* **1992**, *96*, 4931.
(18) Nevoral, V.; Votrubová, V.; Hasal, P.; Schreiberová, L.; Marek, M. *J. Phys. Chem. A* **1997**, *101*, 4954.
(19) Muñuzuri, A. P.; Perez-Muñuzuri, V.; Gomez-Gesteira, M.; Chua, L. O. *Int. J. Bifurcation Chaos* **1995**, *5*, 17.
(20) Booth, V.; Erneux, T. *Physica A* **1992**, *188*, 206.
(21) Erneux, T.; Nicolis, G. *Physica D* **1993**, *67*, 237.
(22) Pazó, D.; Montejo, N.; Pérez-Muñuzuri, V. *Phys. Rev. E* **2001**, *63*, 066206.
(23) Kladko, K.; Mitkov, I.; Bishop, A. R. *Phys. Rev. Lett.* **2000**, *84*, 4505.
(24) Fáth, G. *Physica D* **1998**, *116*, 176.
(25) Bressloff, P. C. *Physica D* **2001**, *155*, 83.
(26) Field, R. J.; Noyes, R. M. *J. Chem. Phys.* **1974**, *60*, 1877.
(27) Field, R. J.; Köros, E.; Noyes, R. M. *J. Am. Chem. Soc.* **1972**, *94*, 8649.
(28) De Donder, T. *L'Affinité*; Gauthier-Villars: Paris, 1928.
(29) Meixner, J.; Reik, H. G., Thermodynamik der irreversiblen Prozesse in *Handbuch der Physik*; Flügge, S., Ed.; Springer: Berlin, 1959; Vol. 3.
(30) Prigogine, I. *Thermodynamics of Irreversible Processes*, 3rd ed.; Interscience: New York, 1967.
(31) de Groot, S. R.; Mazur, P. *Nonequilibrium Thermodynamics;* North-Holland: Amsterdam, 1962.
(32) Clausius, R. *Ann. Phys. (Leipzig)* **1865**, *125*, 355.
(33) Eu, B. C. *Chem. Phys. Lett.* **1988**, *143*, 65.
(34) Gyorgyi, L.; Turanyi, T.; Field, R. J. *J. Phys. Chem.* **1990**, *94*, 7162.
(35) Hindmarsh, A. C. *Livermore Solver for Ordinary Differential Equations*, Technical Report No. UCID-3001; Lawrence Laboratory, Livermore, CA, 1972.
(36) Gear, C. W. *Numerical Initial Value Problems in Ordinary Differential Equations*; Prentice-Hall: Englewood Cliffs, NJ, 1971.
(37) Al-Ghoul, M.; Eu, B. C. *Physica D* **1996**, *90*, 119.
(38) Al-Ghoul, M.; Eu, B. C. *Physica D* **1996**, *97*, 531.